Beware of the Simulated DAG! Varsortability in Additive Noise Models

Alexander G. Reisach^{1,2}, Christof Seiler^{2,3}, and Sebastian Weichwald¹

¹Department of Mathematical Sciences, University of Copenhagen, Denmark
 ²Department of Data Science and Knowledge Engineering, Maastricht University, The Netherlands
 ³ Mathematics Centre Maastricht , Maastricht University , The Netherlands

February 2021

Abstract

Additive noise models are a class of causal models in which each variable is defined as a function of its causes plus independent noise. In such models, the ordering of variables by marginal variances may be indicative of the causal order. We introduce varsortability as a measure of agreement between the ordering by marginal variance and the causal order. We show how varsortability dominates the performance of continuous structure learning algorithms on synthetic data. On real-world data, varsortability is an implausible and untestable assumption and we find no indication of high varsortability. We aim to raise awareness that varsortability easily occurs in simulated additive noise models. We provide a baseline method that explicitly exploits varsortability and advocate reporting varsortability in benchmarking data.

1. Introduction

Causal structure learning is concerned with inferring a causal model from data. Causal models are of interest across academic disciplines anywhere from biology, medicine, finance, to machine learning [Rothman et al., 2008, Imbens and Rubin, 2015, Sanford and Moosa, 2012, Schölkopf, 2019]. They model not only the observational joint distribution of variables but also formalize how to predict the effects of interventions and counterfactuals [Spirtes et al., 2000, Pearl, 2009, Peters et al., 2017]. The data-generating causal structure is commonly represented by a directed acyclic graph (DAG). The nodes represent variables and the directed edges pointing from cause to effect represent the causal relationships. This graphical representation rests on strong assumptions which have been critically questioned, for example, by Dawid [2010]. Here, we consider the task of inferring a linear additive noise model from observational data. Inferring causal structure from observational data is difficult: Often we can only identify the DAG up to its Markov equivalence class and identifying high-scoring DAGs is NP-hard [Chickering, 1996, Chickering et al., 2004].

We focus on the role of data scale for learning the causal structure of linear additive noise models. Multiple prior works contain implicit or explicit statements on this matter. The structure identified by ICA-LiNGAM [Shimizu et al., 2006] is susceptible to rescaling of the variables. This motivated the development of DirectLiNGAM [Shimizu et al., 2011], a scale-invariant causal discovery algorithm for linear non-Gaussian models. Peters and Bühlmann [2014] prove that the causal structure of a linear causal model with Gaussian noise is identifiable if the error variances are equal or known. Any unknown re-scaling of the data breaks this condition and yields the general Gaussian case. For the case of linear structural causal models, Loh and Bühlmann [2014] provide a framework for DAG estimation based on a variance-weighted least squares score function. Given an additive noise model, they also show conditions under which the general Gaussian case can be identified via approximating it by the equal variance case. Yet, re-weighting requires knowledge of the (approximate) true data scale. Weichwald et al. [2020] provide empirical evidence that on the true data scale, raw regression coefficients may carry more information about the causal structure than p-values, an insight they successfully leveraged to win the NeurIPS Causality 4 Climate competition with ordinary regression-based methods [Runge et al., 2020]. Finally, Park [2020] shows that the causal structure is identifiable under certain regularity conditions on the conditional variances along the causal ordering; in particular, identifiability holds if the nodes' error variances are weakly monotone increasing along the causal order. Yet, such identifiability results only hold on the true data scale and thus requires knowledge about it.

In this article, we explain how data scale affects continuous causal structure learning algorithms. Such algorithms optimize model fit under a differentiable acyclicity constraint [Zheng et al., 2018]. This allows for the use of continuous optimization and avoids the explicit traversal of possible causal structures. This idea has found numerous applications and extensions such as those by Lachapelle et al. [2019], Lee et al. [2019], Ng et al. [2020], Yu et al. [2019], Brouillard et al. [2020], Pamfil et al. [2020], Wei et al. [2020], Zheng et al. [2020]. We argue that the data scale of the observed variables invariably affects the identification of stationary points by the first and second order optimization procedures of continuous structure learning algorithms. Leveraging the global causal information in the data scale helps continuous structure learning algorithms achieve state-ofthe-art results. Data standardization, as commonly performed during data preprocessing, or an unknown data scale remove this information and strongly diminish per-

Causal structure learning via continuous optimization requires the choice of a score function. Ideally, the score function is such that its optimum consistently identifies the causal structure while retaining some flexibility against model misspecification. To this end, Loh and Bühlmann [2014] propose a re-weighted mean squared error (MSE) loss function. It can, given knowledge of the noise variances, provably identify the causal graph of additive noise models irrespective of the noise distributions. As we typically lack such knowledge for real-world data, NOTEARS [Zheng et al., 2018] and GOLEM [Ng et al., 2020] revert to assessing the model fit on the raw data scale. While NOTEARS is based on the MSE, GOLEM assesses model fit by the penalized likelihood assuming a jointly Gaussian model. On simulated data and across noise types, both methods recover graphs that are remarkably close to the ground truth causal graph in structural intervention distance (SID) and structural hamming distance (SHD). We agree with the original authors that these empirical findings, especially under model misspecification, may seem surprising at first. Here, we investigate the performance under data standardization and explain how common synthetic benchmarking set-ups yield settings in which the causal order is (approximately) identifiable from the data scale alone.

1.1. Motivating Example

To showcase the role of the data scale in structure learning, we show that re-scaling observations can render the graph unidentifiable. We consider the simple causal graph $A \to B$ as a minimal representative example. To compare models, we use the MSE as a loss function. Consider the data generating process

$$A = N_A$$

$$B = wN_A + N_B \tag{1}$$

where w is non-zero and $N_A \sim \mathcal{U}_A$ and $N_B \sim \mathcal{U}_B$ are independent noise variables for some distributions \mathcal{U}_A and \mathcal{U}_B with mean 0. Given this causal structure, we wish to compare the two models M1) $A \rightarrow B$ and M2) $A \leftarrow B$ with respect to their MSE. It holds that

MSE
$$(M1)$$
 < MSE $(M2)$ \iff Var (A) < Var (B) \iff $(1 - w^2)$ Var (N_A) < Var (N_B)

(see Appendix A).

Problem Deciding the directionality of the edge between A and B based on the MSE amounts to inferring an edge from the lower-variance variable to the higher-variance variable. In fact, the settings in which this marginal-variance-based orientation rule correctly recovers the edges in the true underlying causal graph are the ones we characterize by our notion of varsortability (cf. Section 3.1). For error variances $Var(N_A) \leq Var(N_B)$ we have Var(A) < Var(B) for any non-zero edge weight w and thus the MSE-based inference is sure to be correct whenever $Var(N_A) \leq Var(N_B)$. This resembles known scale-based identifiability results based on equal or monotonously increasing error variances [Peters and Bühlmann, 2014, Park, 2020]. However, if the values of A were multiplied with a sufficiently large constant, the MSE of M1, the correct causal model, would be greater than that of M2. MSE-based inference would then wrongfully conclude that $A \leftarrow B$. This is problematic as we may be changing the variance just by choosing our units of measurement differently. Arguably, this is often the case for observations from real-world systems. From a causal perspective, there is no canonical choice as to whether we should pick meters or yards for distances, gram or kilogram for weights, yuan or dollar for currency; importantly, our inference about whether travel distance and weight of goods are causes of postage rates ought to be independent of such choices. Presently, a researcher applying any method that leverages the data scale (such as, for example, Peters and Bühlmann [2014], Zheng et al. [2018], Ng et al. [2020], Park [2020] and some of their derivatives) cannot rely on obtaining the same results for different measurement scales or after re-scaling the data. Finding the correct data scale, for which the identifiability assumptions may be met, constitutes an acute problem for the practical applicability of scale-dependent structure learning algorithms.

It may not be surprising that some structure learning algorithms fail to recover the true graph when rescaling variables. We expose that causal structure drives the marginal variances of nodes in an additive noise model. This insight opens the door towards exploiting data scale if knowledge about the noise terms or the true data scale is available, just as identifiability can be proven under equal or monotone increasing error variances [Peters et al., 2014, Park, 2020]. Conversely, scale-dependency of a causal structure learning algorithm constitutes a problem for real-world settings in which no such knowledge is

available. Our findings suggest causal structure learning benchmarks should be explicit about either providing information about the data scale (for example by not scaling or standardizing observations), or actively removing data scale information to mimick a real-world setting without such information.

1.2. Contribution

We examine the impact of causal information in the data scale due to compounding additive noise on causal structure learning algorithms. We observe that some continuous algorithms perform orders of magnitude better on the original data scale than on standardized data. We find that increasing marginal variance along the causal order can lead to (partial) identifiability. We introduce varsortibility as a measure of how much information the data scale carries about the causal structure and show that common simulation settings exhibit high varsortability. We explain how varsortability affects continuous structure learning algorithms and is responsible for their state-of-the-art performance. We provide a baseline algorithm built specifically to exploit the causal information in the data scale. We further compare all algorithms on real-world data and do not find a dominating algorithm. We conclude by outlining promising research avenues to leverage our findings for the design of future structure learning algorithms and suitable benchmarks. In an attempt to foster reproducibility and future extensions, we release the code for our experiments under an open source license.

Outline In Section 2, we recap additive noise models and known identifiability results. We briefly introduce the structure learning algorithms that we compare in our experiments. We introduce varsortability in Section 3 as a measure of agreement between a partial ordering induced by the causal structure and the ordering induced by marginal node variances. We discuss how continuous structure learning algorithms exploit varsortability and support our claim that marginal variances drive performance of continuous structure learning algorithms via extensive simulation and real-world experiments in Sections 4 and 5, respectively. Section 6 relates our findings to benchmarking and the assumptions underlying additive noise models.

2. Causal Structure Learning in Linear Additive Noise Models

2.1. Model Class

We assume that a dataset X is generated by an acyclic linear additive noise model. Individual observations are denoted by $x^{(i)} \in \mathbb{R}^d$ where $x_j^{(i)}$ denotes the i^{th} i.i.d. observation of the j^{th} dimension of $X = [X_1, ..., X_d]^\top$. All observations are stacked as $\mathbf{X} = [x^{(1)}, ..., x^{(n)}]^\top \in \mathbb{R}^{n \times d}$ and

 $x_j \in \mathbb{R}^n$ refers to the j^{th} column of X. Analogously, $n^{(i)}$ denotes the corresponding i.i.d. observation of the noise vector $N = [N_1, ..., N_d]^{\top}$, which has zero-centred independent components. The linear effect of variable X_k on X_j is denoted by $w_{k \to j} = w_{kj}$. The causal structure corresponding to the adjacency matrix $W = [w_{kj}]_{k,j=1,...,d}$ with columns $w_j = [w_{k \to j}]_{j=1,...,d} \in \mathbb{R}^d$ can be represented by a directed acyclic graph $G = (V_G, E_G)$ with vertices $V_G = \{1, ..., d\}$ and edges $E_G = \{(k, j) : w_{k \to j} \neq 0\}$. Edges can be represented by an adjacency matrix E such that the $(k, j)^{\text{th}}$ entry of E^l is non-zero if and only if a directed path of length l from k to j exists in G. For a given graph, the parents of j are denoted by PA (j). The structural causal model can be expressed as $X = W^{\top}X + N$.

2.2. Identifiability of Additive Noise Models

Identifiability of the causal structure or an equivalence class thereof requires causal assumptions. In this section we summarise conditions that are sufficient for the graph or its equivalence class of an additive noise model to be identifiable from the observational distribution. Under causal faithfulness and Markov assumptions, the causal graph can be recovered up to a Markov-equivalence class [Chickering, 1995, Spirtes et al., 2000]. Faithfulness, however, is untestable [Zhang and Spirtes, 2008]. Shimizu et al. [2006] show that under the assumption of no unobserved confounders, faithfulness, linearity, and non-Gaussian noise, the causal graph can be recovered from data. Hoyer et al. [2009] show that this holds for any kind of noise under the assumption of strict nonlinearity. This finding is generalized to post-nonlinear functions by Zhang and Hyvarinen [2012]. In the case of Gaussian causal noise with equal (or known) error variances, Peters and Bühlmann [2014] show that the DAG is identifiable from the joint distribution. If the node variances are known, Loh and Bühlmann [2014] show that a re-weighted least squares score can recover the true DAG. Park [2020] shows that monotonously increasing or decreasing conditional node variances also lead to structure identifiability for general additive noise models.

2.3. Structure Learning Algorithms

Combinatorial structure learning algorithms solve the combinatorial problem of finding the true DAG and the problem of finding the correct parameters separately. To remain computationally feasible, the search space of potential structures is often restricted or traversed according to a heuristic. This can, for example, be accomplished by carefully choosing which conditional independence statements to evaluate in constraint-based algorithms, or by greedy (equivalence class) search in score-based algorithms. In our experiments, we consider *PC* [Spirtes and Glymour, 1991], *FGES* Meek [1997], Chickering [2002], and *DirectLiNGAM* [Shimizu et al., 2011]. For details see Appendix F.

Continuous structure learning algorithms employ continuous optimization to simultaneously optimize over structures and parameters. As a first step towards expressing causal structure learning as a continuous optimization problem, Aragam and Zhou [2015] propose l^1 -regularization instead of the conventional l^0 -penalty for model selection. Zheng et al. [2018] propose a differentiable acyclicity constraint, allowing for end-to-end optimization of score functions over graph adjacency matrices. In the following sections we examine and compare the continuous structure learning algorithms NOTEARS [Zheng et al., 2018] and GOLEM [Ng et al., 2020]. For details see Appendix F.

NOTEARS [Zheng et al., 2018] minimizes the MSE between observations and model predictions subject to a hard acyclicity constraint. The MSE with respect to W on observations X is defined as

$$MSE_{\mathbf{X}}(W) = \|\mathbf{X} - \mathbf{X}W\|_{2}^{2}$$
.

GOLEM [Ng et al., 2020] performs maximum likelihood estimation (MLE) under the assumption of a multivariate Gaussian distribution with equal (EV) or non-equal (NV) noise variances. The ojective function is penalized by a soft acyclicity and a sparsity penalty. The likelihood-part of the objective is given as

$$\mathcal{L}_{EV}(W, \mathbf{X}) = \log(\mathrm{MSE}_{\mathbf{X}}(W)), \text{ or}$$

$$\mathcal{L}_{NV}(W, \mathbf{X}) = \sum_{j=1}^{d} \log \left(\|x_j - \mathbf{X}w_j\|_2^2 \right).$$

To ease notation, we sometimes drop the explicit mention of the data matrix X when referring to MSE, \mathcal{L}_{EV} , \mathcal{L}_{NV} .

3. Varsortability

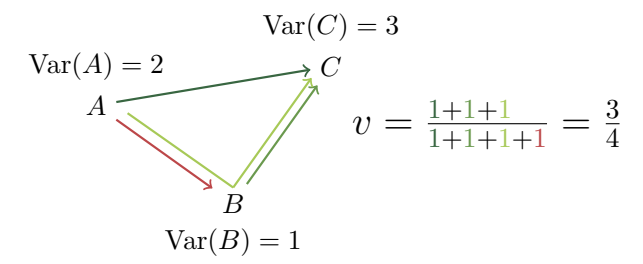
In this section we present how the data-generating process leaves information about the causal order in the data scale. We introduce varsortability as a measure of such information. When varsortability is maximal, the causal order is identifiable. We show that varsortability is high in common simulation schemes for benchmarking causal structure learning algorithms. This explains, at least partially, the results of continuous methods reported by Zheng et al. [2018], Ng et al. [2020], and others. As these algorithms perform global updates, they can leverage the global signal of the marginal variances increasing along the causal order and are susceptible to data rescaling. We introduce sortnregress as a baseline method that systematically exploits the data scale and thereby discloses to what extent scale information drives structure learning on given dataset.

3.1. Definition of Varsortability

We propose varsortability as a measure of agreement between the ordering by marginal variance and the causal order. For any causal graph G = (V, E) over variables $V = \{X_1, ..., X_d\}$, we define varsortability as the fraction of directed paths of any length which start from a node with strictly lower variance than the node they end in, that is.

$$v := \frac{\sum_{k=1}^{d-1} \sum_{i \to j \in E^k} \mathbf{1}[\text{Var}(X_i) < \text{Var}(X_j)]}{\sum_{k=1}^{d-1} \sum_{i \to j \in E^k} \mathbf{1}} \in [0, 1].$$

Consider the following illustration:



Varsortability equals one if the marginal variance of each node is strictly greater than that of its causal ancestors. Varsortability equals zero if the marginal variance of each node is greater than that of its causal descendants. The definition of varsortability does not depend on choosing one of the possibly multiple causal orders and enables us to capture the overall agreement between the partial order induced by the marginal variances and all pathwise descendant relations implied by the causal structure.

We return to our motivational example (cf. Equation (1)). In this two-node model, if varsortability v = 1, then

$$Var(A) < Var(B) \iff Var(N_A) < w^2 Var(N_A) + Var(N_B)$$

where *A* and *B* are nodes in the causal graph $A \stackrel{w}{\rightarrow} B$ and $Var(N_A)$, $Var(N_B)$ are the corresponding noise variances.

Varsortability can be understood as a property of the distribution from which graphs and parameters are sampled. As such, varsortability is of concern for synthetic benchmarking settings. If the weights and noise variances are drawn at random, the distributions they are drawn from determine the probability of obtaining varsortability for each individual connected node pair in the graph. Even for modest chances of varsortability between any two neighboring nodes, the variance of nodes along the causal order increases quickly. The further apart a pair of nodes along the chain, the greater the chance their ordering by variance corresponds to the causal order. In practice, for many instantiations of additive noise models there are high chances an ordering of nodes by marginal variance is closer to the causal ordering than a random ordering (cf. Appendix C).

3.2. Varsortability and Identifiability

If varsortability v = 1, the causal structure is identifiable. It can be recovered by ordering the nodes by increasing marginal variance and regressing each node

onto its predecessors using conventional sparse regression approaches. While closely related, the identifiability conditions in Park [2020] are not equivalent to varsortability, which we prove in Appendix B. Decoupling the causal structure learning problem into causal order estimation and parent selection is not uncommon in the literature. It is warranted since we only need the causal ordering to consistently estimate interventional distributions (cf. e.g. [Bühlmann et al., 2014, Section 2.6]). Parent selection is concerned with pruning the fully-connected DAG for previously identified order to identify the causal structure.

While identifiability of the causal order is immediate if varsortability v=1, it shares severe drawbacks with other identifiability conditions that rely on data scale Peters and Bühlmann [2014], Loh and Bühlmann [2014], Park [2020]. First, it is difficult to verify or assess the plausibility of such assumptions for any given dataset, even if variables are on the same measurement scale. Second, any unknown rescaling may break previously met identifiability conditions which is an impediment to real-world applications.

3.3. Varsortability in Benchmarking Scenarios

For real-world data we cannot readily assess the extent to which varsortability holds as we do not know the true data scale of the data-generating process. When benchmarking causal structure learning algorithms, however, we can evaluate varsortability for the simulated DAGs and parameter settings. Whether any two nodes in a graph connected by a directed path have increasing variance along that path depends on the distributions of edge weights, noise variances, and adjacency matrices. We may acquire some intuition about how probable it is to encounter varsortable cause-effect pairs in our simulation settings by considering the following example: Let A and B be any two nodes in the sampled graph with edge $A \stackrel{w}{\rightarrow} B$ and without any common ancestors and no other directed path from A to B. We can bound the probability for the variable pair (A, B) to be varsortable from below as per

$$P[\operatorname{Var}(A) < \operatorname{Var}(B)]$$

$$= P\left[\operatorname{Var}(A) < \operatorname{Var}\left(wA + \sum_{X \in \operatorname{PA}(B) \setminus \{A\}} w_{X \to B}X + N_B\right)\right]$$

$$\geq P[\operatorname{Var}(A) < \operatorname{Var}(wN_A + N_B)]$$

$$= P[(1 - w^2)\operatorname{Var}(N_A) < \operatorname{Var}(N_B)]$$

In particular, all variable pairs with $w \ge 1$ satisfy this condition if noise variances are non-zero. In the common experimental settings used by, for example, Zheng et al. [2018, 2020], Lachapelle et al. [2019], Ng et al. [2020], weights $w \in [a,b]$, and standard deviations of the noise terms $\operatorname{sd}(N_A), \operatorname{sd}(N_B) \in [c,d]$ are bounded and uniformly distributed. For $w \sim \operatorname{Unif}((-2,-0.5) \cup$

(0.5, 2)) (as, for example, in Zheng et al. [2018], Ng et al. [2020]), and $sd(N_A)$, $sd(N_B) \sim Unif((0.5, 2))$ we have $P[Var(A) < Var(wN_A + N_B)] \approx 0.93$. Empirically, we find that varsortability averages above 0.94 in our simulated graphs and above 0.71 in commonly considered non-linear additive noise models (cf. Appendix C). This result is indicative of how often varsortability may hold in settings simulated for benchmark experiments. If A and B have a common ancestor or mediator C, which tends to be improbable in commonly simulated sparse graphs, the effect of *C* on *B* may either compound or partially cancel out the effect of A on B. In practice, the effect commonly increases the variance of the effect node B, which may be attributed to the independent sampling of path coefficients which also renders faithfulness violations improbable [Meek, 1995]. We find varsortability to increase with graph density and the lower bound presented above to be loose. In general, when simulating additive noise models we advocate to evaluate the varsortability of the simulated graphs empirically (cf. Appendix C.3 for the implementation). We emphasize that even for varsortability < 1, where identifiability of the causal order is no longer guaranteed, experimental results may still be largely driven by the overall agreement between increasing marginal variance and causal order. The extent to which varsortability may distort experimental comparisons is demonstrated in Section 4.

3.4. Gradients under Varsortability

In this section we provide evidence that varsortability may dominate the performance of continuous structure learning algorithms. Intuitively, the effect of varsortability as a global attribute is amplified in continuous algorithms which perform global updates and mitigated in combinatorial ones which perform local updates. We therefore neither expect PC, as local constraint-based algorithm, nor *FGES*, as locally greedy score-based search, nor DirectLiNGAM, a procedure minimising residual dependence, to be dependent on the data scale. In contrast to combinatorial score-based methods, which traverse the space of possible causal structures and optimize the parameters for each individually, continuous causal structure learning algorithms involve global simultaneous updates of the graph structure and its parameters. Therefore, we consider it most instructive to explore how varsortability manifests in the gradients of NOTEARS and GOLEM, instead of discussing other scale-invariant methods.

We show how varsortability affects the gradients of score functions that assume equal noise variances and initialise with the empty graph $0_{d\times d}$. Since ∇ MSE (W) \propto $\mathbf{X}^{\top}(\mathbf{X}-\mathbf{X}W)$ we have that ∇ MSE $(0_{d\times d})$ \propto $\mathbf{X}^{\top}\mathbf{X}$ and $\nabla \mathcal{L}_{EV}(0_{d\times d})$ \propto $\log(\mathbf{X}^{\top}\mathbf{X})$ where the logarithm is applied element-wise. The initial gradient step of both *NOTEARS* and *GOLEM-EV* is symmetric. From the next step onward, the symmetry is broken. We have ∇ MSE(W) \propto $[\mathbf{X}^{\top}(x_1-\mathbf{X}w_1),...,\mathbf{X}^{\top}(x_d-\mathbf{X}w_d)]$ where the j^{th} column

 $\mathbf{X}^{\top}(x_j - \mathbf{X}w_j)$ reflects the vector of empirical covariances of the j^{th} residual vector $x_j - \mathbf{X}w_j$ with each x_i . Provided a small identical learning rate was used across all entries of W in the first step, we expect the residuals after the first gradient step to be larger in those components that have higher marginal variance. As a result, the entries in the gradient column $\mathbf{X}^{\top}(x_j - \mathbf{X}w_j)$ are larger for those x_j with higher marginal variance. This leads to bigger gradient steps for edges pointing in the direction of high-variance nodes. Given high varsortability, this corresponds predominantly to the causal direction. This way, the global information about the causal order due to varsortability is effectively exploited.

For *GOLEM-NV*, the marginal variances lead the gradients differently. Letting $MSE_j(w_j) = ||x_j - Xw_j||_2^2$, we have

$$\nabla \mathcal{L}_{NV}(W) \propto \left[\frac{1}{\mathrm{MSE}_{j}\left(w_{j}\right)} \log \left(\mathbf{X}^{\mathsf{T}}(x_{j} - \mathbf{X}w_{j})\right) \right]_{j=1,\dots,d}$$

such that the logarithmic derivative breaks the symmetry of the first step for the non-equal variance formulation of *GOLEM*. We have $\nabla \mathcal{L}_{NV}(0_{d\times d}) \propto \log(\mathbf{X}^{\mathsf{T}}\mathbf{X}) \operatorname{diag}(\|\mathbf{x}_1\|_2^{-2}\dots,\|\mathbf{x}_d\|_2^{-2})$. Although mitigated by the log-term, the column-wise inverse MSE scaling leads to bigger gradient steps for edges pointing in the direction of low-variance nodes. Given high varsortability, this corresponds predominantly to the anti-causal direction.

We focus on the first optimization steps to explain a) why continuous structure learning algorithms that assume equal noise variance work remarkably well in the presence of high varsortability and b) why performance changes once data is standardized and the marginal variances no longer hold information about the causal order. We conjecture that the first gradient steps have a dominant role in determining the causal structure, even though afterwards the optimization is governed by a nontrivial interplay of optimizer, model fit, constraints, and penalties. Because of the acyclicity constraint, it may be enough for a weight $w_{i\rightarrow j}$ to be greater than its counterpart $w_{i\rightarrow i}$ early on in the optimization for the smaller edge to be pruned from there on. For a discussion of the interplay between sparsity penalties and data scale, we defer the reader to Appendix E, which indicates that the nodes need to be on a comparable data scale for l^1 penalization to be well calibrated. We defer the reader to Ng et al. [2020] for a comprehensive discussion of sparsity and acyclicity constraints in continuous DAG learn-

3.5. *sortnregress*: A Baseline to Reveal Varsortability

We propose a baseline algorithm *sortnregress* performing the following two steps:

order search Sort nodes by increasing marginal variance.

parent search Regress each node on all of its predecessors in that order, using a sparse regression technique to prune edges. The recommended and implemented choice is Lasso regression [Tibshirani, 1996] using the Bayesian Information Criterion [Schwarz, 1978] for model selection.

As a baseline, *sortnregress* is easy to implement (cf. Appendix D.1) and highlights and evaluates to which extent the data scale is informative of the causal structure in different benchmark scenarios. An extension for non-linear additive models is readily obtained by using an appropriate non-linear regression technique in the parent search step, possibly paired with cross-validated recursive feature elimination. It facilitates a clear and contextualized assessment of different structure learning procedures in different scenarios. The presence of varsortability and performance of sortnregress add an important dimension which current benchmarks do not consider.

4. Simulations

We compare the performance of the algorithms introduced in Section 2.3 on raw and standardized synthetic data. In our comparison, we distinguish between settings with different noise distributions, graph types, and graph sizes. Our experimental set-up closely follows those in Zheng et al. [2018], Ng et al. [2020] and we contribute results obtained repeating their experiments in Appendix G.

4.1. Data Generation

We sample Erdös-Rényi (ER) [Erdős and Rényi, 1960] and Scale-Free (SF) [Barabási and Albert, 1999] graphs and the parameters for additive noise models according to the simulation details in Table 1. For a graph specified as ER-k or SF-k with d nodes, we simulate dk edges. Our set-up follows Zheng et al. [2018], Ng et al. [2020]. For every combination of parameters, we create a raw data instance and a standardized version that is de-meaned and re-scaled to unit variance. Re-scaling may increase or decrease varsortability and thus be benign or adversarial for the performance of causal structure learning algorithms that exploit data scale or assumptions on the noise variances. Standardization resembles a canonical scaling choice and is a common pre-processing step in the analysis of data if no knowledge about the data or error scale is available. On standardized data, we have varsortability v = 0 and the marginal variances hold no information about the causal ordering of the nodes. In all our experimental settings, varsortability averages above 0.94 on the raw data scale (cf. Appendix C.1).

Repetitions	10
Graphs	ER-2, SF-2, SF-4
Edge weights	i.i.d. Unif $((-2,5) \cup (.5, 2))$
Noise distributions	Exponential, Gaussian, Gumbel
Noise	i.i.d. Unif (.5, 2) (all noise types)
standard deviations	all equal to 1 (Gaussian only)
Nodes	$d \in \{10, 30, 50\}$
Samples	n = 1000

Table 1.: Parameters for the generation of synthetic data.

4.2. Evaluation

We evaluate performance using structural intervention distance (SID) [Peters and Bühlmann, 2015] and structural Hamming distance (SHD) between the recovered graph and ground truth. SID assesses in how far the recovered structure enables to correctly predict the effect of interventions. SHD measures the distance between the true and recovered graph by counting how many edge insertions, deletions, and reversals are required to turn the former into the latter. Since interventional distributions can consistently be estimated given only the causal ordering [Bühlmann et al., 2014], SID is less susceptible to arbitrary choices of edge pruning procedures and thresholds than SHD. Intuitively, SID prioritizes the causal order, while SHD prioritizes the correctness of individual edges.

Following Zheng et al. [2018], Ng et al. [2020], we perform thresholding for the continuous structure learning algorithms and prune edges with an edge weight in the recovered adjacency matrix of less than 0.3. If the returned graph is not acyclic, we iteratively remove the edge with the smallest magnitude weight until all cycles are broken. We find that the qualitative performance differences between raw and standardized data are robust to a wide range of threshold choices. For more details, see Appendix G.

4.3. Performance on Raw versus Standardized Data

Based on the considerations in Section 2, we group our algorithms into combinatorial and continuous algorithms. sortnregress serves as a baseline. We indicate its performance on standardized data as "randomregress", since it amounts to choosing a random order and regressing each node on its predecessors. We use boxplots aggregating the performance achieved in the 10 repetitions on raw and standardized data by each algorithm and create separate plots per noise type to account for identifiability and MLE specification differences. We show the results obtained for ER-2 graphs with 50 nodes and Gaussian noise with non-equal variances in Figure 1 and Figure 2. These results are representative of the results obtained for different graphs and noise distributions (cf. Appendix G).

We observe that combinatorial algorithms are less scale-sensitive than continuous algorithms or the sort-

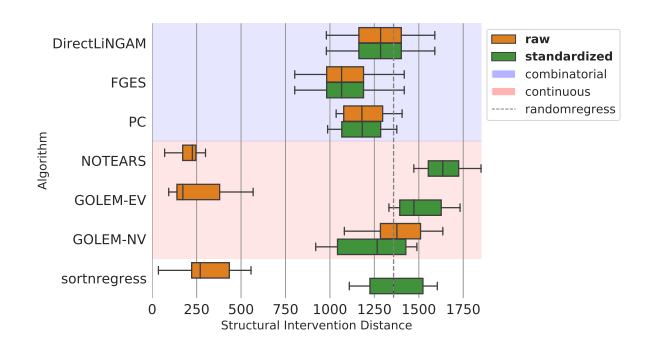


Figure 1.: SID (lower is better) between recovered and ground-truth graphs for ER-2 graphs with 50 nodes and Gaussian-NV noise. The performance of the continuous methods mirrors *sort-nregress*, which only exploits varsortability.

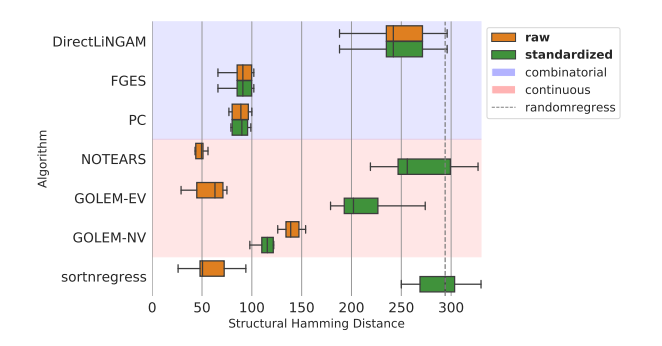


Figure 2.: SHD (lower is better) between recovered and ground-truth graphs for ER-2 graphs with 50 nodes and Gaussian-NV noise. The performance of the continuous methods mirrors sort-nregress, which only exploits varsortability.

nregress baseline, which perform vastly different on raw and standardized data. For the simulated settings, varsortability is high (> 0.94) on the raw data scale (cf. Appendix C.1). sortnregress achieves competitive performance on raw and baseline performance on standardized data. It thus qualifies as a benchmark method to highlight how much of a given causal structure learning task can be resolved by exploiting data scale and sorting nodes by their marginal variance. The performance of NOTEARS and GOLEM-EV, which both assume equal noise variances, follows the same pattern. They perform remarkably well on raw data, but drop below randomregress on standardized data. The performance of Golem-NV is also scale-sensitive but improves upon standardization. This behavior is as predicted by our gradient analysis in Section 3.4. In light of this evidence, the remarkable performance on raw data and the overall behavior upon standardization of the continuous structure learning algorithms appear to be driven by varsortability.

5. Evaluation on Real-World Data

We analyze a dataset on protein signaling networks obtained by Sachs et al. [2005]. We evaluate our algorithms on ten bootstrap samples of the observational part of the dataset consisting of 853 observations, 11 nodes, and 17 edges.

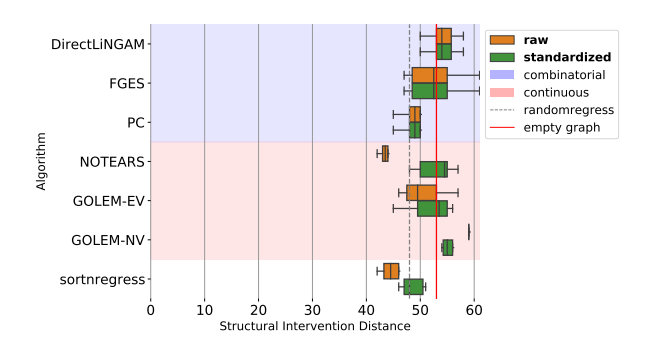


Figure 3.: SID performance of combinatorial and continuous methods on real-world data.

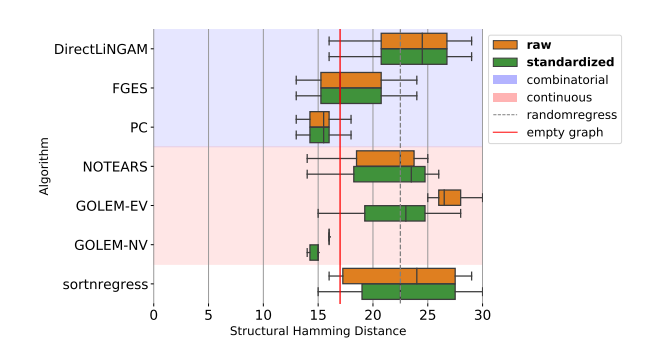


Figure 4.: SHD performance of combinatorial and continuous methods on real-world data.

Our results show that there is no dominating algorithm. In Figure 3 and Figure 4 we see that, on average, most algorithms achieve performances similar to those of *randomregress* or the empty graph baseline. Note that the results in terms of SHD are susceptible to thresholding choices, given that the empty graph baseline outperforms a majority of the algorithms. Our results are in line with previous reports in the literature [Lachapelle et al., 2019, Ng et al., 2020]. We observe scale-sensitivity of the continuous learning algorithms and *sortnregress*. However, in contrast to our simulation study in Section 4, the effect is small and inconsistent. The results do not show the patterns observed under high varsortability, indicating that varsortability is low or absent in this dataset.

6. Discussion and Conclusion

We find that continuous structure learning methods are highly susceptible to data rescaling and some do not perform well without access to the true data scale. Therefore, scale-variant causal structure learning methods should be applied and benchmarked with caution, especially if the variables do not share a measurement scale or when the true scale of the data is unattainable. It is important to declare whether data is being standardized prior to being fed to various structure learning algorithms.

Our aim is to raise awareness of the severity with which scaling properties in data from simulated DAGs and causal additive models may distort algorithm performance. Increasing marginal variances can render scenarios identifiable, which may commonly not be expected to be so—for example the Gaussian case with non-equal variances. We therefore argue that varsortability should be taken into account for future benchmarking. Yet, with any synthetic benchmark there remains a risk that the results are not indicative of algorithm performance on real data. Our results indicate that current structure learning algorithms may perform within the range of naive baselines on real-world datasets.

Varsortability arises in many additive noise models and the marginal variances increase drastically along the causal order, at least in common simulation settings. This begs the question whether this phenomenon can also be observed in nature, and if not, how applicable the additive noise assumption is in practice. The critical examination of the validity or plausibility of the additive noise assumption for real-world data might help guide future research in causal structure learning.

Acknowledgements

We thank Jonas M. Kübler, Jonas Peters, and Sorawit Saengkyongam for helpful discussions and comments. SW was supported by the Carlsberg Foundation.

References

- Bryon Aragam and Qing Zhou. Concave penalized estimation of sparse Gaussian Bayesian networks. *Journal of Machine Learning Research*, 16(1):2273–2328, 2015.
- Albert-László Barabási and Réka Albert. Emergence of scaling in random networks. *Science*, 286(5439):509–512, 1999.
- Philippe Brouillard, Sébastien Lachapelle, Alexandre Lacoste, Simon Lacoste-Julien, and Alexandre Drouin. Differentiable causal discovery from interventional data. In *Advances in Neural Information Processing Systems*, volume 33, pages 21865–21877, 2020.
- Peter Bühlmann, Jonas Peters, and Jan Ernest. CAM: Causal additive models, high-dimensional order search and penalized regression. *The Annals of Statistics*, 42(6): 2526–2556, 2014.
- David M. Chickering. A Transformational Characterization of Equivalent Bayesian Network Structures. In *Proceedings of the Eleventh Conference on Uncertainty in Artificial Intelligence (UAI1995)*, page 87–98, 1995.
- David M. Chickering. Learning Bayesian networks is NP-complete. In *Learning from data*, pages 121–130. Springer, 1996.
- David M. Chickering. Optimal structure identification with greedy search. *Journal of Machine Learning Research*, 3(11):507–554, 2002.
- David M. Chickering, David Heckerman, and Chris Meek. Large-sample learning of Bayesian networks is NP-hard. *Journal of Machine Learning Research*, 5, 2004.
- Philip A. Dawid. Beware of the DAG! In *Causality: objectives and assessment*, pages 59–86. PMLR, 2010.
- Paul Erdős and Alfréd Rényi. On the evolution of random graphs. *Publ. Math. Inst. Hung. Acad. Sci*, 5(1):17–60, 1960.
- Patrik Hoyer, Dominik Janzing, Joris M. Mooij, Jonas Peters, and Bernhard Schölkopf. Nonlinear causal discovery with additive noise models. In *Advances in Neural Information Processing Systems*, volume 21, pages 689–696, 2009.
- Guido W. Imbens and Donald B. Rubin. *Causal inference in statistics, social, and biomedical sciences.* Cambridge University Press, 2015.
- Sébastien Lachapelle, Philippe Brouillard, Tristan Deleu, and Simon Lacoste-Julien. Gradient-based neural DAG learning. *arXiv preprint arXiv:1906.02226*, 2019.
- Hao-Chih Lee, Matteo Danieletto, Riccardo Miotto, Sarah T. Cherng, and Joel T. Dudley. Scaling structural learning with no-bears to infer causal transcriptome networks. In *Pac Symp Biocomput*. World Scientific, 2019.

- Po-Ling Loh and Peter Bühlmann. High-dimensional learning of linear causal networks via inverse covariance estimation. *Journal of Machine Learning Research*, 15(1):3065–3105, 2014.
- Christopher Meek. Strong Completeness And Faithfulness In Bayesian Networks. In *Proceedings of Eleventh Conference on Uncertainty in Artificial Intelligence (UAI1995)*, pages 411–418, August 1995.
- Christopher Meek. *Graphical Models: Selecting causal and statistical models.* PhD thesis, Carnegie Mellon University, 1997.
- Ignavier Ng, AmirEmad Ghassami, and Kun Zhang. On the role of sparsity and DAG constraints for learning linear DAGs. Advances in Neural Information Processing Systems, 33, 2020.
- Roxana Pamfil, Nisara Sriwattanaworachai, Shaan Desai, Philip Pilgerstorfer, Konstantinos Georgatzis, Paul Beaumont, and Bryon Aragam. Dynotears: Structure learning from time-series data. In *International Conference on Artificial Intelligence and Statistics*, pages 1595–1605, 2020.
- Gunwoong Park. Identifiability of additive noise models using conditional variances. *Journal of Machine Learning Research*, 21(75):1–34, 2020.
- Judea Pearl. Causal inference in statistics: An overview. *Statistics surveys*, 3:96–146, 2009.
- Jonas Peters and Peter Bühlmann. Identifiability of gaussian structural equation models with equal error variances. *Biometrika*, 101(1):219–228, 2014.
- Jonas Peters and Peter Bühlmann. Structural intervention distance for evaluating causal graphs. *Neural computation*, 27(3):771–799, 2015.
- Jonas Peters, Joris M. Mooij, Dominik Janzing, and Bernhard Schölkopf. Causal discovery with continuous additive noise models. *Journal of Machine Learning Research*, 15(1):2009–2053, 2014.
- Jonas Peters, Dominik Janzing, and Bernhard Schölkopf. *Elements of Causal Inference.* The MIT Press, 2017.
- Joseph D. Ramsey, Kun Zhang, Madelyn Glymour, Ruben S. Romero, Biwei Huang, Imme Ebert-Uphoff, Savini Samarasinghe, Elizabeth A. Barnes, and Clark Glymour. TETRAD—A toolbox for causal discovery. In 8th international workshop on Climate Informatics (CI 2018), 2018.
- Kenneth J. Rothman, Sander Greenland, and Timothy L. Lash. *Modern epidemiology*. Lippincott Williams & Wilkins, 2008.
- Jakob Runge, Xavier-Andoni Tibau, Matthias Bruhns, Jordi Muñoz-Marí, and Gustau Camps-Valls. The causality for climate competition. In *NeurIPS 2019*

- Competition and Demonstration Track, pages 110–120. PMLR, 2020.
- Karen Sachs, Omar Perez, Dana Pe'er, Douglas A. Lauffenburger, and Garry P. Nolan. Causal proteinsignaling networks derived from multiparameter single-cell data. *Science*, 308(5721):523–529, 2005.
- Andrew D. Sanford and Imad A. Moosa. A bayesian network structure for operational risk modelling in structured finance operations. *Journal of the Operational Research Society*, 63(4):431–444, 2012.
- Bernhard Schölkopf. Causality for machine learning. *arXiv preprint arXiv:1911.10500*, 2019.
- Gideon Schwarz. Estimating the dimension of a model. *The annals of statistics*, 6(2):461–464, 1978.
- Shohei Shimizu, Patrik O. Hoyer, Aapo Hyvärinen, and Antti Kerminen. A linear non-gaussian acyclic model for causal discovery. *Journal of Machine Learning Research*, 7:2003–2030, 2006.
- Shohei Shimizu, Takanori Inazumi, Yasuhiro Sogawa, Aapo Hyvärinen, Yoshinobu Kawahara, Takashi Washio, Patrik O. Hoyer, and Kenneth Bollen. Directlingam: A direct method for learning a linear non-gaussian structural equation model. *Journal of Machine Learning Research*, 12:1225–1248, 2011.
- Peter Spirtes and Clark Glymour. An algorithm for fast recovery of sparse causal graphs. *Social science computer review*, 9(1):62–72, 1991.
- Peter Spirtes, Clark N. Glymour, Richard Scheines, and David Heckerman. *Causation, prediction, and search.* MIT press, 2000.
- Robert Tibshirani. Regression shrinkage and selection via the lasso. *Journal of the Royal Statistical Society: Series B (Methodological)*, 58(1):267–288, 1996.
- Dennis Wei, Tian Gao, and Yue Yu. DAGs with No Fears: A Closer Look at Continuous Optimization for Learning Bayesian Networks. *arXiv preprint arXiv:2010.09133*, 2020.
- Sebastian Weichwald, Martin E. Jakobsen, Phillip B. Mogensen, Lasse Petersen, Nikolaj Thams, and Gherardo Varando. Causal structure learning from time series: Large regression coefficients may predict causal links better in practice than small p-values. In *NeurIPS 2019 Competition and Demonstration Track*, pages 27–36. PMLR, 2020.
- Yue Yu, Jie Chen, Tian Gao, and Mo Yu. DAG-GNN: DAG structure learning with graph neural networks. *arXiv* preprint arXiv:1904.10098, 2019.
- Jiji Zhang and Peter Spirtes. Detection of unfaithfulness and robust causal inference. *Minds and Machines*, 18 (2):239–271, 2008.

- Kun Zhang and Aapo Hyvarinen. On the identifiability of the post-nonlinear causal model. *arXiv* preprint *arXiv*:1205.2599, 2012.
- Xun Zheng, Bryon Aragam, Pradeep K. Ravikumar, and Eric P. Xing. DAGs with NO TEARS: Continuous optimization for structure learning. In *Advances in Neural Information Processing Systems*, pages 9472–9483, 2018.
- Xun Zheng, Chen Dan, Bryon Aragam, Pradeep K. Ravikumar, and Eric P. Xing. Learning sparse non-parametric DAGs. In *International Conference on Artificial Intelligence and Statistics*, pages 3414–3425. PMLR, 2020.

A. Varsortibility in the Two-Node Case

Consider the following ground-truth and two competing linear acyclic models:

Ground truth model: Model M1) " $A \rightarrow B$ ": Model M2) " $A \leftarrow B$ ":

$$A := N_A$$
 $\widehat{A} = 0$ $\widehat{A} = \widehat{v}B$ $B := wN_A + N_B$ $\widehat{B} = \widehat{w}A$ $\widehat{B} = 0$

where $w \neq 0$, N_A and N_B are independent zero-centred noise terms that follow some distributions with non-vanishing variance V_A and V_B , respectively, and $\widehat{w} = \frac{\text{Cov}(A,B)}{\text{Var}(A)} = w$ and $\widehat{v} = \frac{\text{Cov}(A,B)}{\text{Var}(B)} = \frac{wV_A}{\text{Var}(B)}$ are the corresponding ordinary least-squares linear regression coefficients.

We evaluate when the true model *M1* obtains a smaller MSE than the wrong model *M2*, to decide if and under which conditions a MSE-based orientation rule recovers the ground-truth edge direction:

$$\text{MSE } (M1) < \text{MSE } (M2)$$

$$\text{Var}(A) + \text{Var}(B - \widehat{w}A) < \text{Var}(A - \widehat{v}B) + \text{Var}(B)$$

$$\Leftrightarrow \qquad \text{Var}(A) + \text{Var} \left((wN_A + N_B) - wN_A \right) < \text{Var} \left(N_A - \frac{wV_A}{\text{Var}(B)} (wN_A + N_B) \right) + \text{Var}(B)$$

$$\Leftrightarrow \qquad \qquad V_A + V_B < \frac{V_A V_B}{\text{Var}(B)} + w^2 V_A + V_B$$

$$\Leftrightarrow \qquad \qquad 0 < V_A \left(\frac{V_B}{\text{Var}(B)} - 1 \right) + w^2 V_A$$

$$\Leftrightarrow \qquad \qquad 0 < \frac{-w^2 V_A}{\text{Var}(B)} + w^2$$

$$\Leftrightarrow \qquad \qquad V_A < \text{Var}(B)$$

$$\Leftrightarrow \qquad \qquad (1 - w^2) V_A < V_B$$

B. Varsortability and Identifiability by Conditional Noise Variances

While closely related, varsortability is not equivalent to the identifiability conditions laid out in Theorem 4, Park [2020], (henceforth referred to as "Theorem 4"). We prove this by providing two examples. In 1) part A) of the conditions in Theorem 4 is satisfied, while varsortability does not hold. In 2) varsortability holds but neither part A) nor part B) of Theorem 4 are satisfied.

1) Park, 2020, Theorem 4 conditions satisfied without varsortability

Consider the following ground-truth model with unique causal order *A*, *B*, *C*:

$$A := N_A$$

$$B := \beta_{A \to B} A + N_B = 1A + N_B$$

$$C := \beta_{B \to C} B + N_C = \sqrt{\frac{2}{3}} B + N_C$$

where N_A , N_B , N_C are jointly independent zero-centred noise terms with respective variances $\sigma_A^2 = 4$, $\sigma_B^2 = 2$, $\sigma_C^2 = 1$. The marginal variances are Var(A) = 4 < Var(C) = 5 < Var(B) = 6. Our example resembles the examples in Section 3.1 of Park [2020]. We can verify the three conditions for part A) of Theorem 4:

$$(A1) \quad \sigma_{A}^{2} < \sigma_{B}^{2} + \beta_{A \to B}^{2} \sigma_{A}^{2}, \qquad (A2) \quad \sigma_{B}^{2} < \sigma_{C}^{2} + \beta_{B \to C}^{2} \sigma_{B}^{2}, \qquad (A3) \quad \sigma_{A}^{2} < \sigma_{C}^{2} + \beta_{B \to C}^{2} \sigma_{B}^{2} + \beta_{A \to B}^{2} \beta_{B \to C}^{2} \sigma_{A}^{2}.$$

Inserting the values from above, we obtain

$$(A1) \quad 4 < 2 + 1 \cdot 4, \qquad (A2) \quad 2 < 1 + \frac{2}{3} \cdot 2, \qquad (A3) \quad 4 < 1 + \frac{2}{3} \cdot 2 + 1 \cdot \frac{2}{3} \cdot 4.$$

Our result verifies that identifiability is given as per Theorem 4 in Park [2020], while the order of increasing marginal variances is not in complete agreement with the causal order and varsortibility is not equal to 1.

2) Varsortability without Park, 2020, Theorem 4 conditions satisfied

Consider the following ground-truth model with unique causal order *A*, *B*, *C*:

$$\begin{split} A &:= N_A \\ B &:= \beta_{A \to B} A + N_B = A + N_B \\ C &:= \beta_{A \to C} A + \beta_{B \to C} B + N_C = \frac{1}{\sqrt{2}} A + \frac{1}{\sqrt{2}} B + N_C \end{split}$$

where N_A , N_B , N_C are jointly independent zero-centred noise terms with respective variances $\sigma_A^2 = 4$, $\sigma_B^2 = 3$, $\sigma_C^2 = 1$. The marginal variances are Var(A) = 4 < Var(B) = 7 < Var(C) = 10.5. We now verify, that for both case A) and B) in Theorem 4 of Park [2020] at least one of the inequality constraints is violated.

One of the three conditions in A) is

$$\sigma_B^2 < \sigma_C^2 + \beta_{B \to C}^2 \sigma_B^2$$

while for the above model we have

$$3 \not< 1 + \frac{1}{2} \cdot 3.$$

One of the three conditions in B) is

$$\frac{\sigma_C^2}{\sigma_B^2} > (1 - \beta_{B \to C}^2),$$

while for the above model we have

$$\frac{1}{3} > (1 - \frac{1}{2}).$$

For both criteria A) and B) in Theorem 4 at least one of the inequalities is not satisfied. We thus verify, that even if identifiability is not given as per the sufficient conditions in Theorem 4, Park [2020], varsortability may still render the causal order identifiable.

C. Empirical Evaluation of Varsortability

We estimate varsortability empirically for our experimental set-up and a nonlinear version of our experimental set-up by calculating the fraction of directed paths that are correctly sorted by marginal variance.

C.1. Varsortability in Linear Additive Noise Models

Consistent with our theoretical results, Table 2 shows that varsortability is close to 1 across all graph and noise types in our experimental set-up. As conjectured, varsortability is higher in denser than in sparser graphs.

		varsortability		
		min	mean	max
graph	noise			
ER-1	Gauss-EV	0.94	0.97	0.99
	exponential	0.94	0.97	0.99
	gumbel	0.94	0.97	1.00
ER-2	Gauss-EV	0.97	0.99	1.00
	exponential	0.97	0.99	1.00
	gumbel	0.98	0.99	0.99
ER-4	Gauss-EV	0.98	0.99	0.99
	exponential	0.98	0.99	0.99
	gumbel	0.98	0.99	0.99
SF-4	Gauss-EV	0.98	1.00	1.00
	exponential	0.98	1.00	1.00
	gumbel	0.98	1.00	1.00

Table 2.: Empirical varsortability in our experimental linear ANM set-up. Average varsortability is high in all settings. Our parameter choices are common in the literature. We sample 1000 observations of ten 50-node graphs for each combination of graph and noise type.

C.2. Varsortability in Non-Linear Additive Noise Models

Table 3 shows a nonlinear version of our experimental set-up as used in Zheng et al. [2020]. While the fluctuations in Table 3 are greater, all settings exhibit high varsortability on average. Our findings indicate that varsortability is a concern for additive noise models more generally.

		varsortability		
		min	mean	max
graph	ANM-type			
ER-1	Additive GP	0.81	0.91	1.00
	GP	0.72	0.86	0.96
	MLP	0.55	0.79	0.96
	Multi Index Model	0.62	0.82	1.00
ER-2	Additive GP	0.79	0.91	0.98
	GP	0.82	0.89	0.97
	MLP	0.46	0.71	0.87
	Multi Index Model	0.65	0.79	0.89
ER-4	Additive GP	0.90	0.95	0.98
	GP	0.74	0.88	0.93
	MLP	0.59	0.72	0.85
	Multi Index Model	0.57	0.73	0.85
SF-4	Additive GP	0.95	0.97	0.99
	GP	0.88	0.94	0.97
	MLP	0.75	0.83	0.93
	Multi Index Model	0.77	0.84	0.97

Table 3.: Empirical varsortability in non-Linear ANM. Average varsortability is high in all settings. Our parameter choices are common in the literature. We sample 1000 observations of ten 20-node graphs for each combination of graph and ANM-type.

C.3. Varsortability Algorithm

```
import numpy as np
def varsortability(X, W):
    """ Takes n x d data and a d x d adjaceny matrix,
    where the i,j-th entry corresponds to the edge weight for i->j,
    and returns a value indicating how well the variance order
    reflects the causal order. ""
   E = W != 0
    Ek = E.copy()
    var = np.var(X, axis=0, keepdims=True)
    tol = var.min() * 1e-9
    n_paths = 0
    n_correctly_ordered_paths = 0
    for k in range(E.shape[0] - 1):
        n_paths += Ek.sum()
        n_correctly_ordered_paths += (Ek * var / var.T > 1 + tol).sum()
        Ek = Ek.dot(E)
    return n_correctly_ordered_paths / n_paths
```

D. Baselines

D.1. Sortnregress

```
import numpy as np
from sklearn.linear_model import LinearRegression, LassoLarsIC
def sortnregress(X):
     """ Take nx d data, order nodes by marginal variance and
    regresses each node onto those with lower variance, using
    edge coefficients as structure estimates. """
    LR = LinearRegression()
    LL = LassoLarsIC (criterion = 'bic')
    d = X. shape[1]
   W = np.zeros((d, d))
    increasing = np.argsort(np.var(X, axis=0))
    for k in range(1, d):
        covariates = increasing[:k]
        target = increasing[k]
        LR.\ fit\ (X[:,\ covariates\,]\,,\ X[:,\ target\,].\ ravel\ ())
        weight = np.abs(LR.coef_)
        LL.fit(X[:, covariates] * weight, X[:, target].ravel())
        W[covariates, target] = LL.coef_ * weight
    return W
```

D.2. Sorting by Variance in Non-Linear Settings

Table 4 shows the results of a crude "sort-by-variance-and-just-fill-in-all-edges" baseline in a nonlinear setting. This is more naive than *sortnregress*. We do not show performance in terms of SHD, as this varsortability-baseline is only considering the fully connected graph. While tthe comparisons are not on the original dataset, we still consider it instructive to observe how well even a crude variance sorting compares to more involved methods. This sorting by variance performs substantially better than a random graph, and plain variance-sorting or *sortnregress* may therefore be much more informative baselines than random graphs.

This begs the question, how much GraN-DAG, or other successful methods, exploit varsortability, and how they perform under standardization. We encourage such an exploration in future work and suggest that varsortability and (a nonlinear version of) *sortnregress* should always be included in future benchmarks.

	varsortability	SID when sorting by variance	SID obtained by GraN-DAG	SID of random graph
graph-type				
ER-4	0.90	180.20 ± 12.27	165.1 ± 21.0	298.5 ± 28.7
SF-4	0.96	74.00 ± 8.96	62.5 ± 18.8	204.8 ± 38.5

Table 4.: Naive baseline in non-linear setting. 1000 observations of ER-4 and SF-4 Gauss-ANM 20 node graphs. Comparison to GraN-DAG and random baseline as in Lachapelle et al. [2019] (Table 8, A.6).

E. Model Selection in Continuous Optimization

Below we show the optimization landscape for the Gaussian MLE estimator under Gaussian-EV noise. We compare vanilla MLE to MLE with Lasso regularization for raw and standardized data. In Figure 5 we show the loss landscape in terms of SID and SHD difference to the true structure and highlight global optima. In the case of tied scores between the true structure and an alternative structure we select the true structure. For MLE with Lasso regularization using a penalty of 0.1, the optimal loss is achieved by the true structure more frequently under standardization (red dots accumulate in the bottom left corner). Our result indicates that the Lasso sparsity penalty is influenced by the data scale and is better calibrated on standardized data. It is not unexpected that penalization is scale dependent, a problem that is, for example, discussed in applications of Ridge regression.

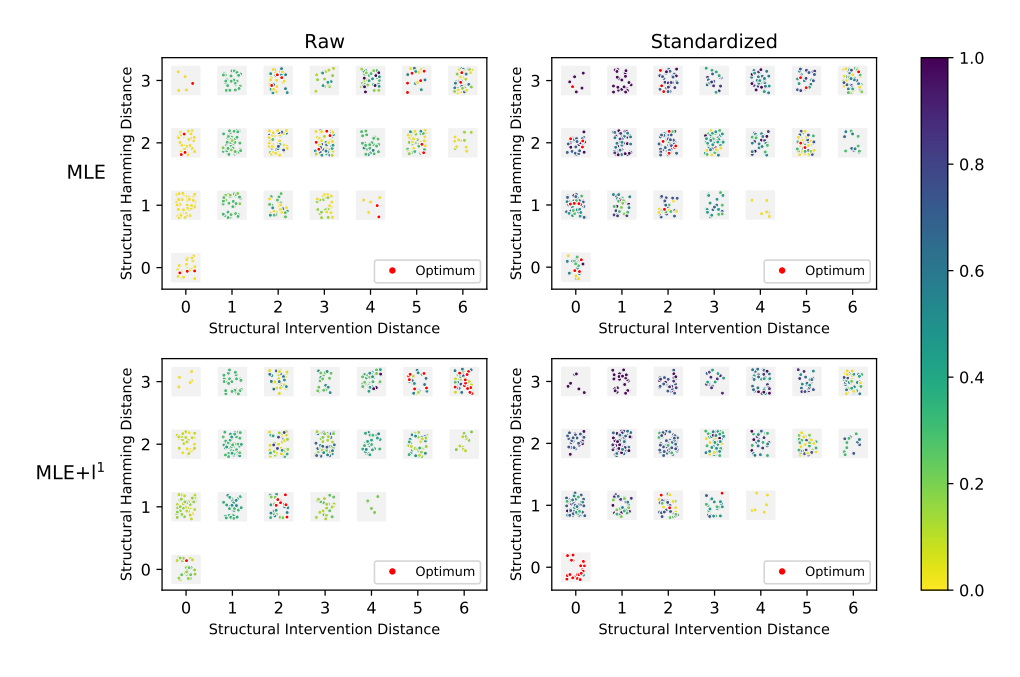


Figure 5.: Standardized loss landscape for all 25 candidate graphs for each of the 25 different 3-node graph structures.

F. Algorithms

DirectLiNGAM is a direct method for learning linear non-Gaussian acyclic models [Shimizu et al., 2011]. It recovers the causal order by iteratively selecting the node whose residuals are least dependent on any predecessor node. In a strictly non-Gaussian setting, *DirectLiNGAM* is guaranteed to converge to the optimal solution asymptotically within a small fixed number of steps and returns a DAG. We use the implementation provided by the authors¹. We deliberately keep the default of a least angle regression penalized by the Bayesian Information Criterion. We find that this penalty strikes a good balance between SID and SHD performance. Cross-validated least angle regression performs better in terms of SID but poorer in terms of SHD.

PC [Spirtes and Glymour, 1991] is provably consistent in estimating the Markov equivalence class of the true data-generating graph if the causal Markov and faithfulness assumptions hold. The algorithm returns a completed partially directed acyclic graph (CPDAG). For computational reasons, we refrain from computing the lower and upper bounds of the SID for comparing CPDAGS with the ground truth DAG as proposed by Peters and Bühlmann [2015]. Instead, we adopt the approach by Zheng et al. [2018] and resolve bidirectional edges favourably to obtain a DAG. We use the implementation in the *Tetrad*² package Ramsey et al. [2018].

FGES is an optimized version of the fast greedy equivalence search algorithm developed by Meek [1997], Chickering [2002]. Under causal Markov and faithfulness assumptions, it is provably consistent for estimating the Markov equivalence class of the true data-generating graph. The algorithm returns a CPDAG, which we resolve favorably to obtain a DAG. We use the implementation in the $tetrad^3$ package [Ramsey et al., 2018].

NOTEARS is a score-based method that is entirely solvable by continuous optimization [Zheng et al., 2018]. The optimization formulation is based on the mean squared error and includes a sparsity penalty parameter λ and a differentiable acyclicity constraint:

$$\underset{W \in \mathbb{R}^{d \times d}}{\operatorname{argmin}} \quad \operatorname{MSE}_{\mathbf{X}}\left(W\right) + \lambda \|W\|_{1} \quad \text{s.t.} \quad \operatorname{tr}(\exp(W \otimes W)) - d = 0.$$

The algorithm returns a DAG. We use the implementation provided by the authors⁴. Throughout all our experiments we set $\lambda = 0$.

GOLEM combines a soft version of the differentiable acyclicity constraint from Zheng et al. [2018] with a MLE objective [Ng et al., 2020]. The authors propose a multivariate Gaussian MLE for equal (EV) or unequal (NV) noise variances and optimize

$$\underset{W \in \mathbb{R}^{d \times d}}{\operatorname{argmin}} \quad \mathcal{L}(W, \mathbf{X}) - \log(|\det(I - W)|) + \lambda_1 ||W||_1 + \lambda_2 (\operatorname{tr}(\exp(W \otimes W)) - d)$$

where \mathcal{L} is either

$$\mathcal{L}_{EV}(W,\mathbf{X}) = \log(\text{MSE}_{\mathbf{X}}(W)) \quad \text{ or } \quad \mathcal{L}_{NV}(W,\mathbf{X}) = \sum_{j=1}^{d} \log \left(\|x_{j} - \mathbf{X}w_{j}\|_{2}^{2} \right).$$

We use the implementation and hyperparameters provided by the authors⁵. We train for 10⁴ episodes as we found that half of that suffices to ensure convergence. Notably, we do not perform any pretraining for our version of *GOLEM-NV*.

sortnregress is implemented as shown in Appendix D.1. We find that here as well, a least angle regression penalized by the Bayesian Information Criterion strikes a good balance between SID and SHD performance.

https://github.com/cdt15/lingam

²https://github.com/cmu-phil/tetrad

³https://github.com/cmu-phil/tetrad

⁴https://github.com/xunzheng/notears

⁵https://github.com/ignavier/golem

G. Detailed Results

G.1. Results Across Thresholding Regimes

To ensure the effects we observe are constitute a general phenomenon, we evaluate algorithm performance for different thresholding regimes. This is especially critical on standardized data. By re-scaling the data, standardization may impact the correct edge weights between nodes, potentially pushing them outside the thresholding range.

Figure 6 shows performance in terms of SID for different thresholds. Even though the thresholds are orders of magnitude apart, a comparison between Figure 6a and Figure 6b reveals that the relative performances are nearly identical.

Figure 7 shows performance in terms of SHD for two different thresholding regimes. Figure 7a shows performance using *favorable* thresholding. In this regime, the threshold leading to the most favorable SHD performance is applied to each instance individually. Figure 7b shows performance for a fixed threshold of 0.3. A comparison reveals nearly identical relative performances in both cases.

Overall, we observe that the effect of varsortability is present even for the most favorable threshold in case of SHD, and for a wide range of thresholds in case of SID, where computation of a favorable threshold is computationally infeasible.

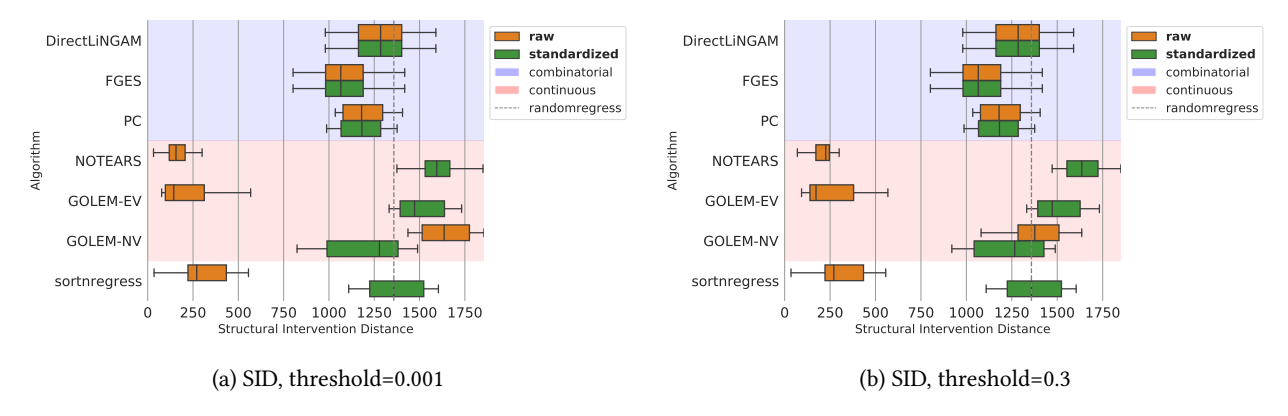


Figure 6.: SID results for different thresholding regimes. Gaussian-NV noise, ER-2 graph, 50 nodes.

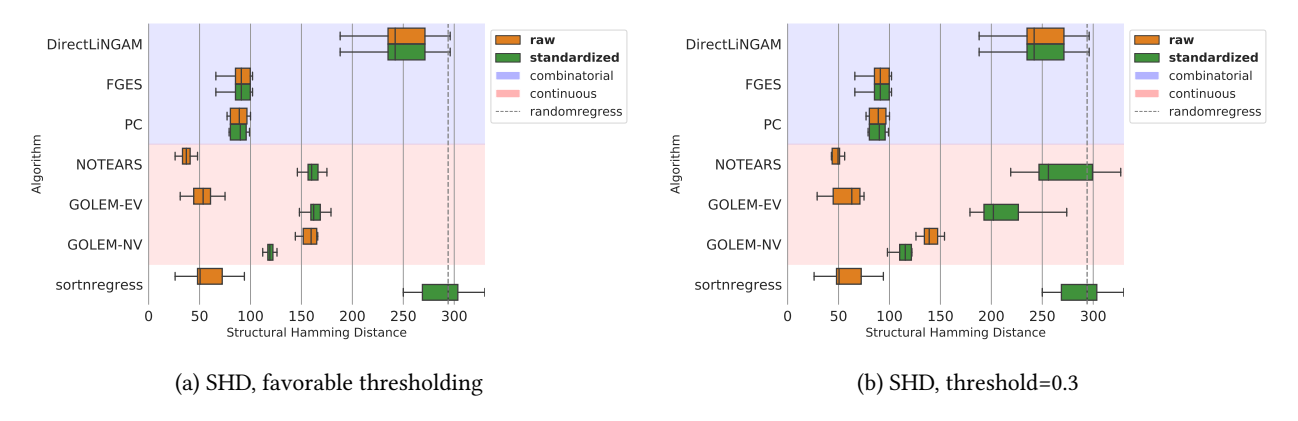


Figure 7.: SHD results for different thresholding regimes. Gaussian-NV noise, ER-2 graph, 50 nodes.

G.2. Results Across Noise Distributions and Graph Types

Figure 8 and Figure 9 show algorithm comparisons in terms of SID and SHD, respectively. We observe qualitatively similar results regardless of the noise distribution and showcase results for different graph types in the non-Gaussian setting. *DirectLiNGAM* performs well only in the non-Gaussian cases, as is expected based on its underlying identifiability assumptions.

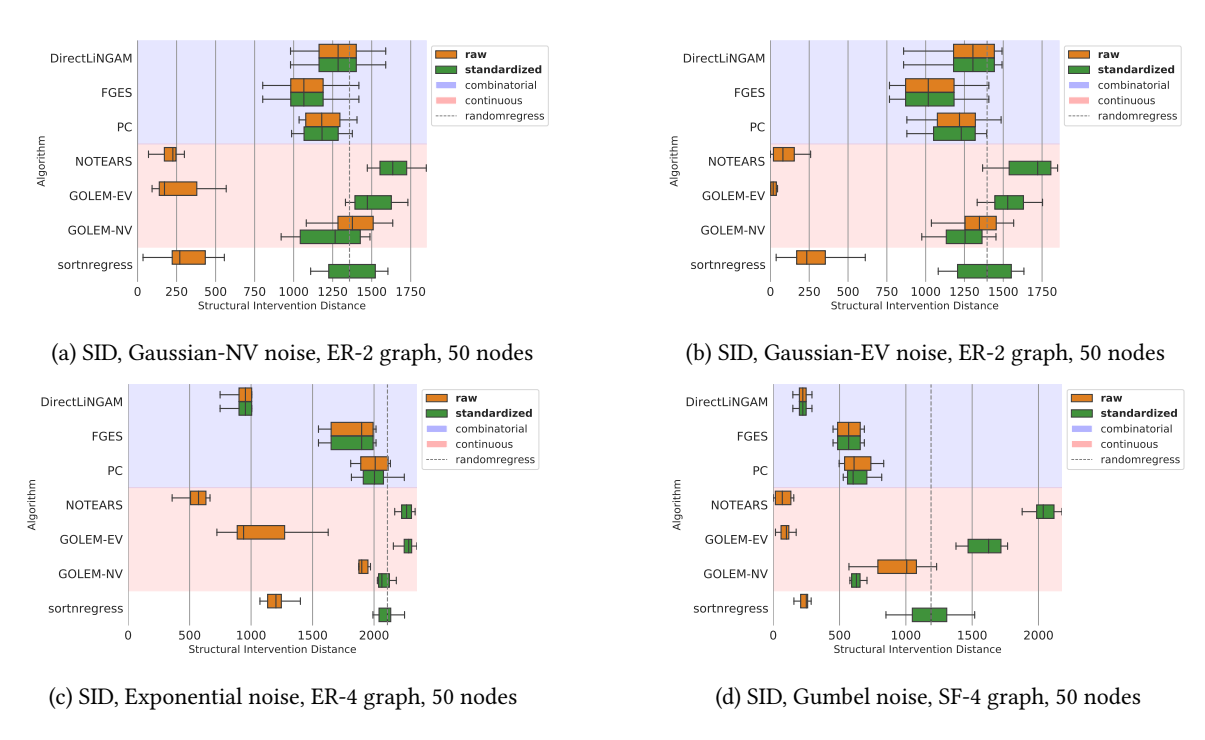


Figure 8.: SID results across noise types and for different graph types with 50 nodes

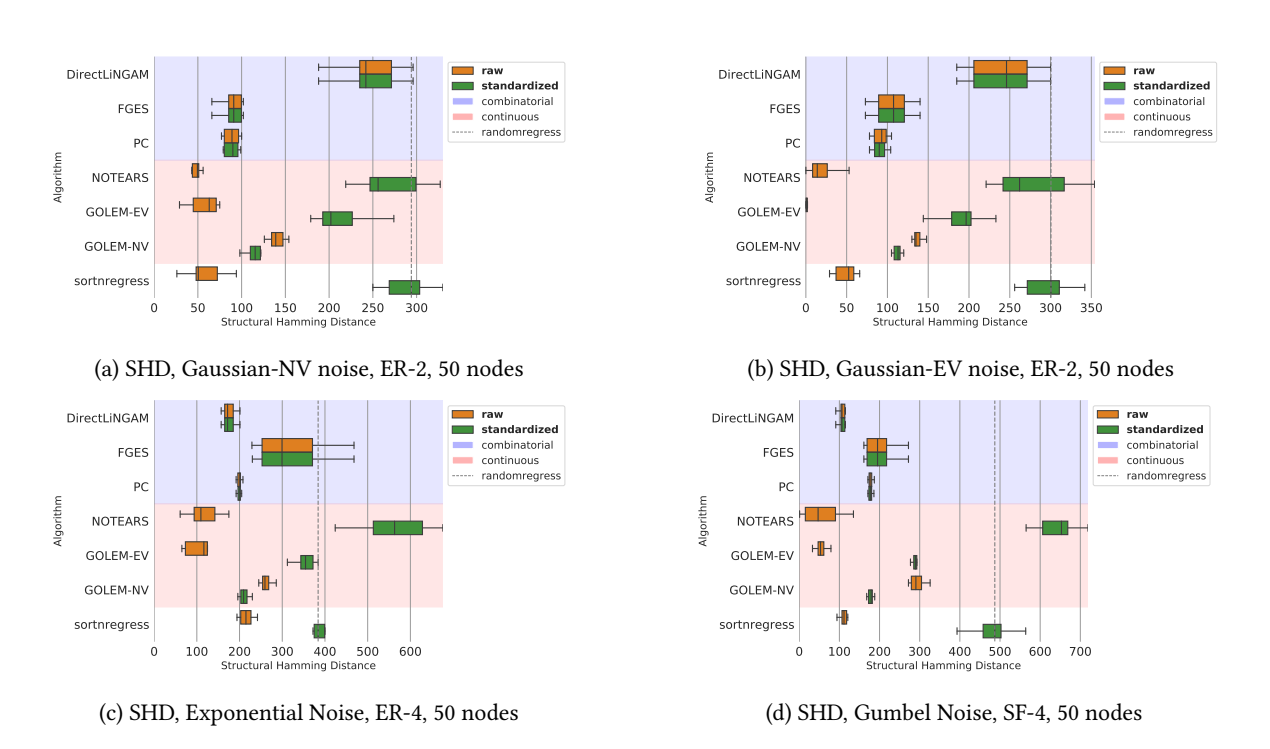


Figure 9.: SHD results across noise types and for different graph types with 50 nodes

G.3. Results Across Noise Distributions, Graph Types, and Graph Sizes

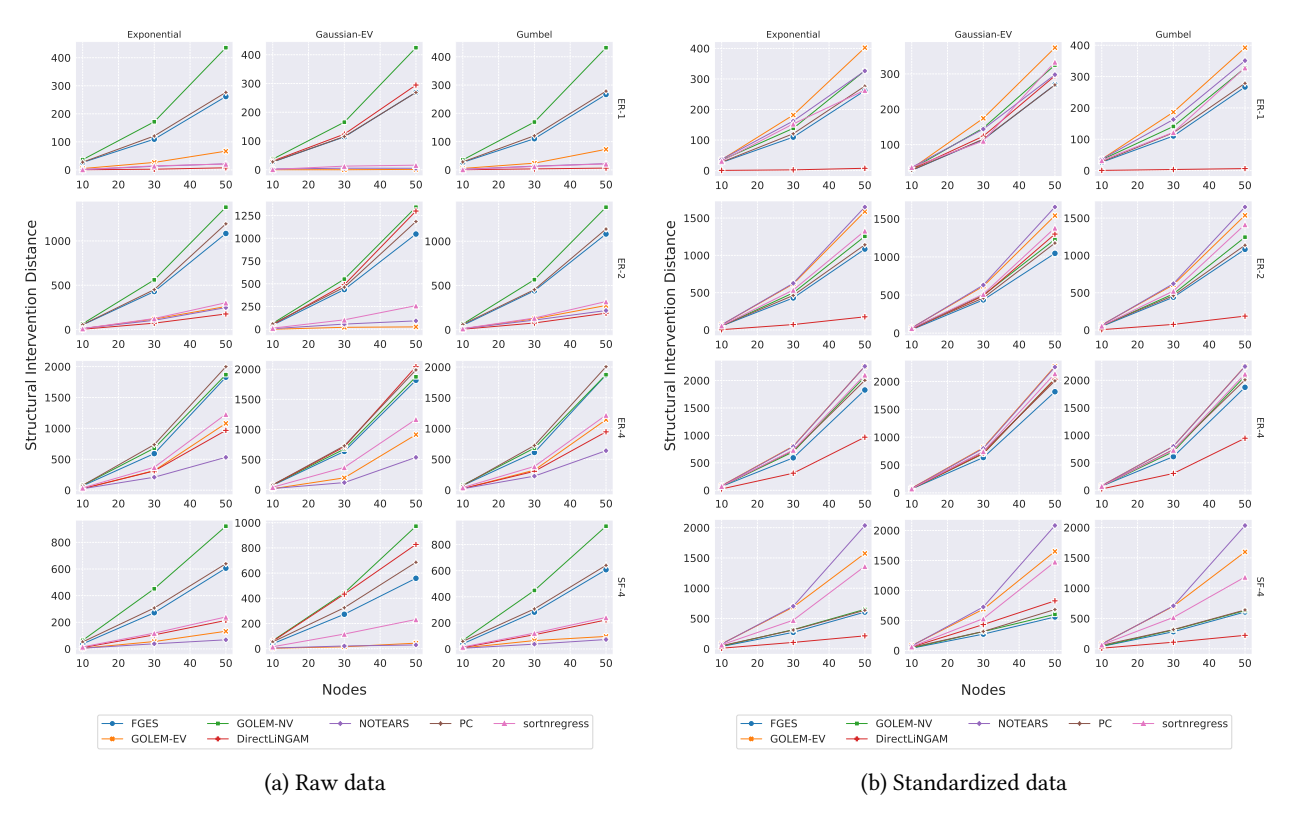


Figure 10.: SID results across noise types, graph types, and graph sizes.

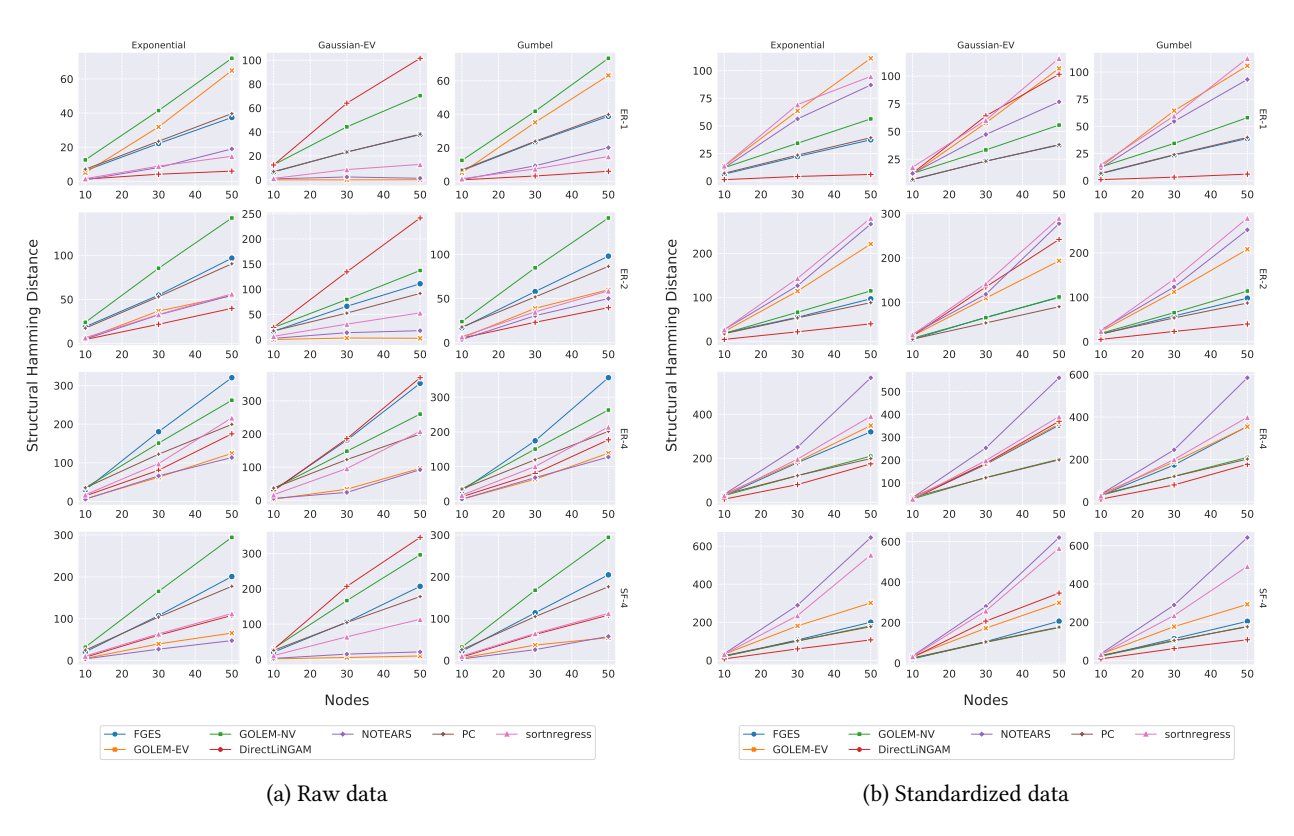


Figure 11.: SHD results across noise types, graph types, and graph sizes.